Mode space in DFTB quantum transport in the nanodevice simulation tool NEMO5

Logan Melican
Department of Electrical and Computer Engineering
Purdue University
West Lafayette, IN
lmelican@purdue.edu

Han-Wei Hsiao
Department of Electrical and Computer Engineering
Purdue University
West Lafayette, IN
hsiao35@purdue.edu

Daniel A. Lemus
Department of Electrical and Computer Engineering
Purdue University
West Lafayette, IN
dlemus@purdue.edu

Tillmann Kubis
Department of Electrical and Computer Engineering
Purdue University
West Lafayette, IN
tkubis@purdue.edu

2024 International Conference on Simulation of Semiconductor Processes and Devices (SISPAD) | 979-8-3315-1635-2/24/$31.00 ©2024 IEEE | DOI: 10.1109/SISPAD62626.2024.10732966

***Abstract* — DFT and DFTB models are preferred representation for quantum transport simulations of nanodevices when atomic features such as defects are considered. This paper showcases NEMO5's new capability to transform nonorthogonal DFT and DFTB models into orthogonal mode space representations, which reduces the numerical costs of DFT-quantum transport and enables the inclusion of virtually all other NEMO5 simulation features.**

Keywords—nanoelectronics, simulation, quantum transport, mode space, DFT, DFTB, NEGF, nanowire

I. Introduction

Today's semiconductor nanodevice modeling is challenged by the advent of new materials and the scaling of interconnects and oxides to their ultimate limits. Predicting the reliability and performance variability of the respective nanodevices requires combining material and defect models with quantum transport simulation capabilities. Exotic material combinations, 2D and 1D materials, irregular interfaces, and point like defects make atomic resolutions in the models essential. Density functional theory (DFT) is commonly accepted as the method of choice for such material and interface challenges. Unfortunately, DFT is computationally unfeasible for frequent solutions of quantum transport on nanometer structures as needed for machine learning based device optimizations [1].

Density-functional based tight binding (DFTB) theory has been applied on systems well beyond 1000 atoms [2] [,3]. It requires a careful, system dependent parameterization to faithfully reproduce DFT results [2]. Quantum transport methods such as the nonequilibrium Green's function method scale roughly cubically with the number of degrees of freedom considered in the system. In spite of DFTB being orders of magnitude faster than DFT, it is still computationally too expensive to be regularly used as basis representation for quantum transport models.

Low rank approximations, such as the mode space method [4], [5] are known to reduce the computational cost of quantum transport simulations by several orders of magnitude – independent of the underlying basis representation. Therefore, the mode space functionality of the multiphysics nanodevice simulation tool NEMO5 has been augmented to solve quantum transport in DFTB representation which is presented in this paper. The underlying implementation creates orthogonal mode space representations, which further reduces the computational burden of the originally nonorthogonal DFTB representation. Thanks to the modularity of NEMO5, the DFTB mode space implementation is fully compatible with all previously reported modeling features of NEMO5.

II. Method

A. DFTB parameterization

The DFTB parameters of any material and interface in the considered nanodevices are fitted to ensure DFTB bandstructure results match DFT results in systems that involve those materials and interfaces but are of DFT compatible size [2]. In systems with deviations from the ideal lattice structure such as at interfaces between materials of different lattice constant, it is critical this fitting process covers all strain and corrugation configurations locally encountered in the considered structures [2]. This ensures transferability of the DFTB parameters to all relevant situations. In this way, the DFTB Hamilton operators for system sizes beyond the limit DFT models can cover with feasible numerical costs are still faithfully reproducing the DFT model's physics. This process is repeated for any material and interface the nanodevice structure contains. This process applies to any chosen DFT functional and is thus applicable to any material and its preferred DFT model.

B. Orthogonalization and rank reduction of basis

Quantum transport calculations are numerically less efficient when solved in nonorthogonal models. Since DFTB is a nonorthogonal model, any DFTB Hamiltonian of a given device is transformed into a device specific, orthogonal basis. This orthogonal basis does not have to offer any transferability to other devices or structures, since it will be approximate in a later step by a lower rank device specific basis set anyways: Mode space representations are known to be device specific [4]. In NEMO5, this orthogonalization step is done with a fitted tight binding Hamiltonian that accurately reproduces the device specific DFTB bandstructure data: The nanodevices are sliced into slabs along the transport direction. For each slab, DFTB Hamiltonian operators are constructed, periodic boundary conditions are applied in transport direction and slab specific

bandstructures as functions of the momentum in transport direction are solved. Those bandstructures are reproduced with an orthogonal, low rank mode space representation following Ref. 4.

C. *Quantum transport features in real space formulation*

Thanks to the modularity of the NEMO5 code structure, the method laid out in the previous sections seamlessly integrates with the well-established transport features of NEMO5. Charge self-consistent solutions of the quantum transport equations with the Poisson equation are unaffected by the newly introduced transformation steps. Similarly, scattering in self-consistent Born approximation on various phonons and charge impurities offers the accuracy and numerical efficiency of the TB models it was originally developed for in NEMO5, since all scattering models are formulated in real-space to which any basis representation can transform to [6], [7]. All other numerical performance features apply to DFTB mode space as well [8]-[11].

III. Results

The new DFTB mode space feature is exemplified on two n-type nanowires: 1) a square [100] grown Si nanowire with a 2x2nm cross section, a centered gate of 5nm length and 1nm thick oxide (see Figs. 1 and 2); 2) a cylindrical, [111] grown Ge nanowire with a 2nm diameter, a centered gate of 5nm length and 1nm thick oxide (see Figs. 3 and 4). The explicitly discretized device section of each nanowire is 16nm long. All nanowire surfaces are passivated with Hydrogen [12].

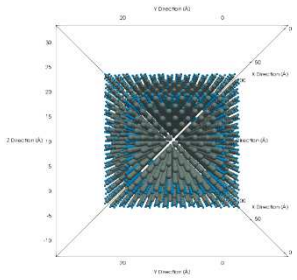

Figure 1 Square [100] grown Si nanowire with a 2x2nm cross section, a centered gate of 5nm length and 1nm thick oxide viewed normal to the transport direction.

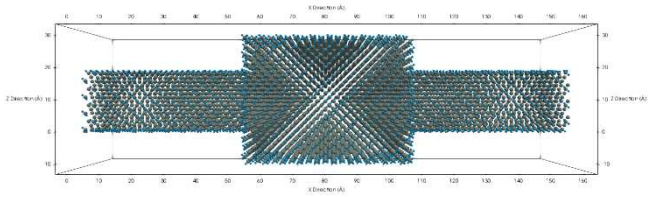

Figure 2 Square Si nanowire of Fig. 1 viewed from the side.

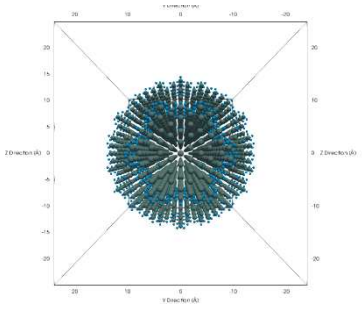

Figure 3 Cylindrical, [111] grown Ge nanowire with a 2nm diameter, a centered gate of 5nm length and 1nm thick oxide Ge nanowire, viewed normal to the transport direction.

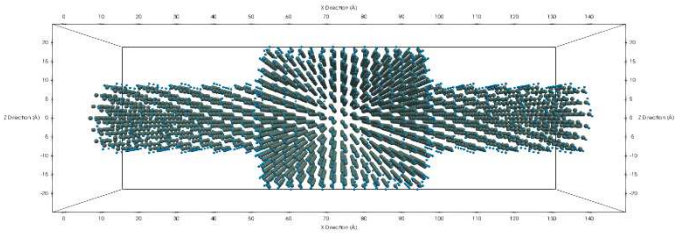

Figure 4 Cylindrical Ge nanowire of Fig. 3 viewed from the side.

A. *Benchmark against full representation/correctness*

Figs. 5 and 6 showcase the agreement of the bulk Si and Ge bandstructures respectively, solved in DFT HSE06 [13] and DFTB+ [14], [15]. Previous work has shown similar agreement for DFT and DFTB+ calculations for a list of 2D materials across all valence bands for a large number of strain configurations [2]. The excellent agreement of DFTB with DFT is the essential for the transferability of the DFTB description to nanodevices.

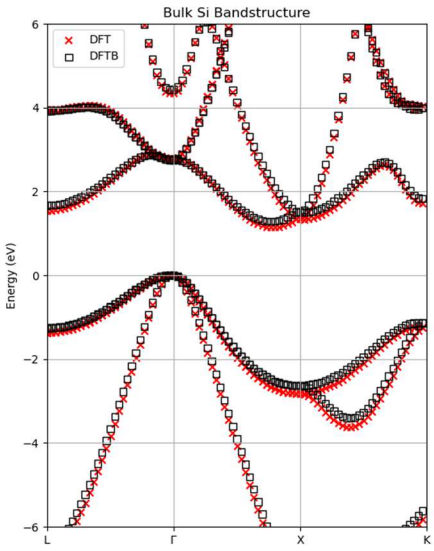

Figure 5 Comparison of band structures of bulk Si obtained using DFT (red) with DFTB (black).

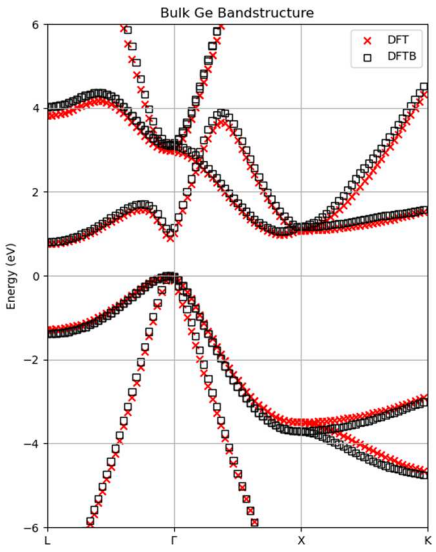

Figure 6 Comparison of band structures of bulk Ge obtained using DFT (red) with DFTB (black).

Fig. 7 compares the DFTB and the low rank approximation mode space conduction bands of a slab of the square Si nanowire. All conduction bands and the spurious state-free bandgap relevant for the operation of the n-type nanowire (for source-drain voltages up to 500mV) are accurately reproduced.

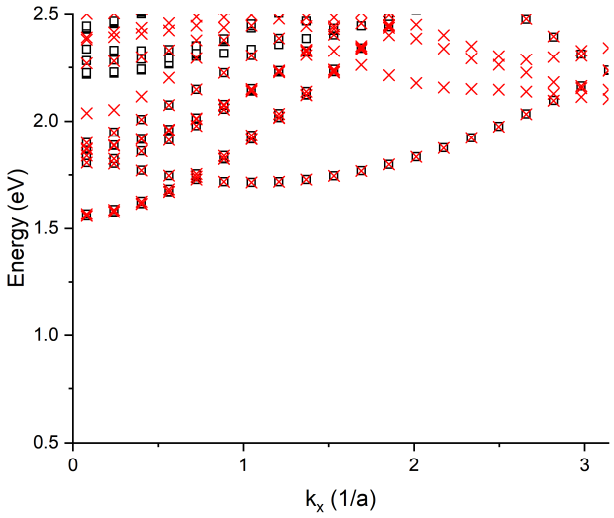

Figure 7 Conduction band states of the Si nanowire of Figs. 1 and 2 for the full basis DFTB Hamitonian (black) compared to those of the reduced basis mode space Hamiltonian (red).

Fig. 8 confirms similar situation for the cylindrical Ge nanowire. NEMO5 offers a systematic workflow for the DFT based mode space approach of any nanowire system.

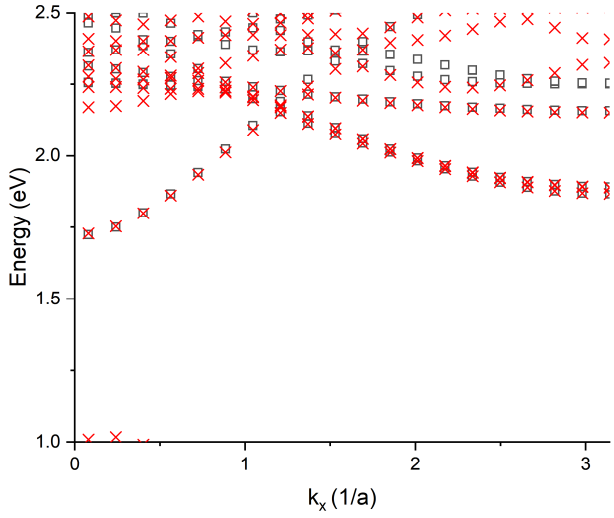

Figure 8 Conduction band states of the Ge nanowire of Figs. 3 and 4 for the full basis DFTB Hamitonian (black) compared to those of the reduced basis mode space Hamiltonian (red).

B. Performance assessment

The numerical complexity of DFT NEGF is significantly higher than the presented DFTB mode space simulations. The degrees of freedom for a DFT-NEGF calculation is assumed to be the number of plane waves used in the DFT calculation. Using a cutoff energy of 500 eV, an HSE06 DFT simulation of the Si nanowire structure is going to use approximately 24 million plane waves. Likewise, a similar DFT simulation of the Ge nanowire structure will use more than 94 million plane waves at a cutoff energy of 550 eV. The orthogonalized DFTB Hamiltonian for the Si nanowire contains only 1,130 basis states, and 1,460 basis states for the Ge nanowire. With a typically cubic complexity of NEGF, using DFTB over DFT yields a speedup factor of approximately 9.7 trillion for Si, and 266.8 trillion for Ge. Applying a low rank approximation to the DFTB Hamiltonian as done in this work yielded a reduced basis of 204 states for Si and 66 states for Ge. This provides an additional speedup by factors of 170 for Si (186 for Ge) resulting in a total speedup vs. the DFT NEGF of 1.65 10^{15}x for the Si nanowire (2.9 10^{18}x for the Ge nanowire).

C. Enabled device simulations

With the beforementioned numerical complexity reduction, current/voltage characteristics of the Si and Ge nanowires of Figs. 1-4 in their DFT-based representation were possible within feasible numerical costs. The calculations ran on 4 nodes of the Negishi community cluster at the Rosen Center for Advanced Computation. With such reduced numerical costs and the modularity of the NEMO5 code base, the inclusion of incoherent scattering on impurities and phonons [6,7], the modeling of electrostatic screening effects of all valence bands [9], and many other simulation features of NEMO5 are easily available for DFT-based nanodevice simulations.

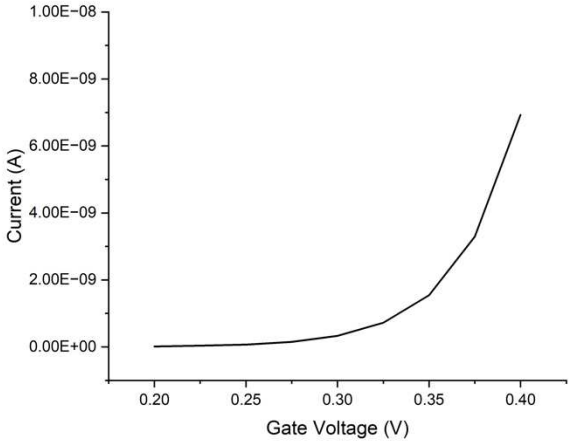

Figure 9 Linear scale I-V characteristics for the Si nanowires of Figs. 1-2.

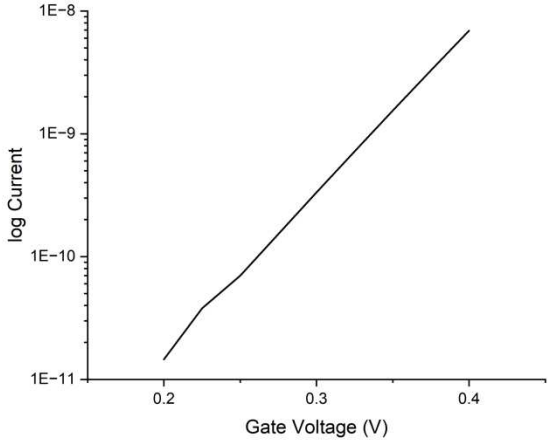

Figure 10 Logarithmic scale I-V characteristics for the Si nanowires of Figs. 1-2.

IV. Conclusion

Mode space calculations of DFT and nonorthogonal DFTB have been demonstrated for 2 types of nanowires, a squared Si and a cylindrical Ge nanowire. The mode space results faithfully reproduce DFT bandstructures and transform the equations into an orthogonal representation. In this way, all previously reported simulation features of NEMO5 are fully compatible with the newly added DFT/DFTB-based mode space representation and simulations in DFTB representation remain cost-efficient in NEMO5.

References

[1] J. Maassen, M. Harb, V. Michaud-Rioux, Y. Zhu, and H. Guo, "Quantum Transport Modeling From First Principles," Proceedings of the IEEE, vol. 101, no. 2, pp. 518–530, Feb. 2013, doi: https://doi.org/10.1109/jproc.2012.2197810.

[2] H.-W. Hsiao, Namita Narendra, and T. Kubis, "Long Range Piezoelectricity Effects in van der Waals Heterobilayer Systems beyond 1000 Atoms," Journal of physics. Condensed matter, vol. 36, no. 26, pp. 265901–265901, Apr. 2024, doi: https://doi.org/10.1088/1361-648x/ad3708.

[3] N. Narendra, X. Chen, J. Wang, J. Charles, R. Graham Cooks, and T. Kubis, "Quantum Mechanical Modeling of Reaction Rate Acceleration in Microdroplets," Journal of Physical Chemistry A, vol. 124, no. 24, pp. 4984–4989, May 2020, doi: https://doi.org/10.1021/acs.jpca.0c03225.

[4] G. Mil'nikov, N. Mori, and Y. Kamakura, "Equivalent transport models in atomistic quantum wires," Physical Review B, vol. 85, no. 3, Jan. 2012, doi: https://doi.org/10.1103/physrevb.85.035317.

[5] D. A. Lemus, J. Charles, and T. Kubis, "Mode-space-compatible inelastic scattering in atomistic nonequilibrium Green's function implementations," Journal of Computational Electronics, vol. 19, no. 4, pp. 1389–1398, Jul. 2020, doi: https://doi.org/10.1007/s10825-020-01549-8.

[6] P. Sarangapani, J. Charles, and T. Kubis, "Tuning Band Tails in Mono- and Multilayered Transition-Metal Dichalcogenides: A Detailed Assessment and a Quick-Reference Guide," Physical Review Applied, vol. 17, no. 2, Feb. 2022, doi: https://doi.org/10.1103/physrevapplied.17.024005.

[7] P. Sarangapani, Y. Chu, J. Charles, G. Klimeck, and T. Kubis, "Band-tail Formation and Band-gap Narrowing Driven by Polar Optical Phonons and Charged Impurities in Atomically Resolved III-V Semiconductors and Nanodevices," Physical review applied, vol. 12, no. 4, Oct. 2019, doi: https://doi.org/10.1103/physrevapplied.12.044045.

[8] Y. Chu et al., "Thermal boundary resistance predictions with non-equilibrium Green's function and molecular dynamics simulations," Applied physics letters, vol. 115, no. 23, Dec. 2019, doi: https://doi.org/10.1063/1.5125037.

[9] Y. Chu, Prasad Sarangapani, J. Charles, G. Klimeck, and T. Kubis, "Explicit screening full band quantum transport model for semiconductor nanodevices," Journal of applied physics, vol. 123, no. 24, Jun. 2018, doi: https://doi.org/10.1063/1.5031461.

[10] K.-C. Wang et al., "Control of interlayer physics in 2H transition metal dichalcogenides," Journal of applied physics, vol. 122, no. 22, Dec. 2017, doi: https://doi.org/10.1063/1.5005958.

[11] S. Steiger, M. Povolotskyi, H.-H. Park, T. Kubis, and G. Klimeck, "NEMO5: A Parallel Multiscale Nanoelectronics Modeling Tool," IEEE Transactions on Nanotechnology, vol. 10, no. 6, pp. 1464–1474, Nov. 2011, doi: https://doi.org/10.1109/tnano.2011.2166164.

[12] Y. He, Y. Tan, Z. Jiang, M. Povolotskyi, G. Klimeck, and T. Kubis, "Surface Passivation in Empirical Tight Binding," I.E.E.E. transactions on electron devices/IEEE transactions on electron devices, vol. 63, no. 3, pp. 954–958, Mar. 2016, doi: https://doi.org/10.1109/ted.2016.2519042.

[13] J. Heyd, G. E. Scuseria, and M. Ernzerhof, "Hybrid functionals based on a screened Coulomb potential," The Journal of Chemical Physics, vol. 118, no. 18, pp. 8207–8215, May 2003, doi: https://doi.org/10.1063/1.1564060.

[14] B. Hourahine et al., "DFTB+, a software package for efficient approximate density functional theory based atomistic simulations," The Journal of Chemical Physics, vol. 152, no. 12, p. 124101, Mar. 2020, doi: https://doi.org/10.1063/1.5143190.

[15] S. Markov, B. Aradi, Chi-Yung Yam, Hang Xie, T. Frauenheim, and Guanhua Chen, "Atomic Level Modeling of Extremely Thin Silicon-on-Insulator MOSFETs Including the Silicon Dioxide: Electronic Structure," IEEE Transactions on Electron Devices, vol. 62, no. 3, pp. 696–704, Mar. 2015, doi: https://doi.org/10.1109/ted.2014.2387288.